

DISCOVERING DOMAIN DISENTANGLEMENT FOR GENERALIZED MULTI-SOURCE DOMAIN ADAPTATION

Zixin Wang, Yadan Luo, Peng-Fei Zhang, Sen Wang, Zi Huang

The University of Queensland, Brisbane 4067, Australia

zixin.wang1@uqconnect.edu.au, {lyadanluo, mima.zpf}@gmail.com, sen.wang@uq.edu.au, huang@itee.uq.edu.au

ABSTRACT

A typical multi-source domain adaptation (MSDA) approach aims to transfer knowledge learned from a set of labeled source domains, to an unlabeled target domain. Nevertheless, prior works strictly assume that each source domain shares the identical group of classes with the target domain, which could hardly be guaranteed as the target label space is not observable. In this paper, we consider a more versatile setting of MSDA, namely Generalized Multi-source Domain Adaptation, wherein the source domains are partially overlapped, and the target domain is allowed to contain novel categories that are not presented in any source domains. This new setting is more elusive than any existing domain adaptation protocols due to the coexistence of the domain and category shifts across the source and target domains. To address this issue, we propose a variational domain disentanglement (VDD) framework, which decomposes the domain representations and semantic features for each instance by encouraging dimension-wise independence. To identify the target samples of unknown classes, we leverage online pseudo labeling, which assigns the pseudo-labels to unlabeled target data based on the confidence scores. Quantitative and qualitative experiments conducted on two benchmark datasets demonstrate the validity of the proposed framework.

Index Terms— Multi-source Domain Adaptation, Category Shift, Domain Disentanglement

1. INTRODUCTION

Due to the heavy dependence on voluminous data for training, the performance of supervised deep learning models will vastly degrade when the labeled data is scarce. To tackle this issue, a possible solution is to combine multiple labeled training datasets (i.e., source domains) to learn a domain-agnostic model for an unlabeled test set (i.e., target domain), which refers to Multi-source Domain Adaptation (MSDA). MSDA allows the source and target data coming from different data distributions, e.g., using images taken from foggy, rainy, and snowy days to classify the ones collected from sunny days.

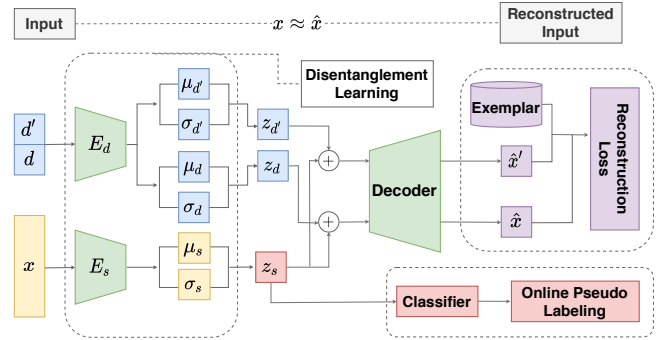


Fig. 1: Variational Domain Disentanglement (VDD).

However, it is challenging to directly apply MSDA into real-world scenarios due to its over-rigorous assumptions on the label space: (1) MSDA requires all source domains to have an identical label set, which could be easily violated in practice. It is highly likely that one source domain may only share *a part of* the classes with another, while the rest of classes are privately preserved; (2) MSDA is commonly under a closed-set setting where the source and target domains are expected to contain the same classes. As the target labels are not available during training, it is more reasonable to consider an *open-set* setting that enables the target domain to contain novel classes that are not presented in any source domains.

In this paper, we relax the label constraint of MSDA and propose a novel yet challenging setting, namely *generalized multi-source domain adaptation* (GMDA). GMDA aims to learn a model from multiple complementary source domains and generalize to the unlabeled target domain with the presence of unknown classes. The core challenge of this task is simultaneously learning to reduce the influence of both category shift (i.e., partially shared source classes and the unknowns in target) and domain shift. Although distribution matching methods [1, 2] or adversarial learning approaches [3] can address the domain shift issue, these prior works could suffer the negative-transfer and class misalignment triggered by unshared categories residing in both the source and target domains.

To address the above issue, we propose a *Variational*

Domain Disentanglement (VDD) framework to bridge both the category and domain gap hidden in visual recognition tasks. Specifically, we design a dual-branch (i.e., paralleled encoders) VAE framework to decompose the representation of each source and target instance into domain-specific and sample-specific features, where only the latter one is used for classification. As illustrated in Fig. 1, the sample and domain encoders (i.e., E_s and E_d) take the raw data and their paired domain labels as input to generate latent vectors, which are then concatenated and passed to the decoder for image reconstruction. We establish two strategies, exemplar learning, and disentanglement learning, to further boost domain disentanglement. For exemplar learning, the model learn to reconstruct the image to resemble an ‘exemplar’ that has the same semantics but a different style as the raw data by replacing the ground-truth domain label of the original data with a ‘fake’ one. Exemplars are randomly selected from each category and source domain, which helps to stabilize the image reconstruction and minimize the intra-domain variance. Regarding the disentanglement learning, we substitute the KL divergence in the evidence lower bound (ELBO) of naïve VAE with total correlation (TC) to learn orthogonal domain representations to gain superior generalization capacity. The disentangled factor learning explicitly reinforces the domain-invariance of the learned sample embedding, which can be more correlated to the intrinsic semantics. In addition, we propose an online pseudo labeling regime to identify the most/least confident target data as the shared known/unknown class to supervise the model in turn. After that, the latent representations of images from the sample encoder can finally become domain-invariant, which then be fed into the classifier for logits. Empirical results show that VDD achieves state-of-the-art performance against existing single-source, multi-source, and open-set domain adaptation methods. Source code is released in the Github repo¹.

2. RELATED WORK

Unsupervised domain adaptation (UDA) studies apply the model trained in a labeled source domain to an unlabeled target domain, where no label information is at one’s disposal. Many challenging applications under different UDA settings [4, 5] were proposed. While more graph based methods can be found at [6, 7]. Multi-source Domain Adaptation (MSDA) typically assumes that the target distribution is a mixture of the source distributions, and search for the optimal combination of the source hypothesis [8]. By considering the existence of category shift, Xu *et al.* [9] proposed Deep Cocktail Network (DCTN), which leverages the K-way adversary to determine the similarity between the source and target domains and re-weights the respective domain-specific classifier. Another stream of work follows the spirit of learn-

ing domain-invariant features by adversarial learning [3] or distribution matching [1, 2, 10] rather than weighting different hypotheses to cope with the domain shift. Han *et al.* [3] extended the domain adversarial neural networks to the multi-source setting. Li *et al.* [2] additionally considered the relationship between source pairs and derived a tighter bound on the weighted multi-source discrepancy. Similarly, Peng *et al.* [10] proposed the MSDA mechanism aligned the moments of feature distributions between each source-source and source-target pair. Wang *et al.* [11] proposed Learning to Combing for Multi-Source Domain Adaptation (Ltc-MSDA), which leverages graph neural networks to propagate cross-domain information within the subgraph for each class. Yang *et al.* [12] re-weighted the source samples by learning a dynamic curriculum, which progressively learns which samples are helpful for adaptation. While the notion of MSDA has been widely exploited in the past, existing algorithms are developed under the strong constraint of label sets for both source and target domains, i.e., assuming each domain has identical sets of classes. Recently, variational disentanglement provides new solutions to large amounts of deep vision tasks [13, 14]. For domain adaptation, Cao *et al.* [15] proposed frameworks with adversarial training to disentangle feature in the latent space. While TLR [16] aims at learning a latent representation to solve the domain shift problem.

3. METHOD

3.1. Problem Formulation and Notations

Multi-source Domain Adaptation (MSDA) aims to transfer a model trained on N labeled source domains $\mathcal{D}_S = \{D_1, D_2, \dots, D_N\}$ to an unlabeled target domain \mathcal{D}_T . Each source domain contains *i.i.d.* sampled data $X_{S_i} = \{x_1, \dots, x_n\}$ with the respective labels $Y_{S_i} = \{y_1, \dots, y_n\} \in \mathcal{Y}$, where \mathcal{Y} is the label space. The ultimate target is to learn a domain-invariant model $f_\theta : \mathcal{X}_T \rightarrow \mathcal{Y}$ parameterized by θ that generalizes the target samples.

Generalized Multi-source Domain Adaptation (GMDA). Different from MSDA which assumes each domain share the same label space $\mathcal{Y} \in \{1, \dots, C\}$, GMDA relaxes this constraint on both sides. Specifically, it allows the source domains to share a part of classes $Y_{ij} = Y_{S_i} \cap Y_{S_j}$ and have the label sets private to the other source domain $\bar{Y}_{ij} = Y_{S_i} \setminus Y_{ij}$. We indicate all source labels $Y_S = \bigcup Y_{S_i}$, and the target label set is a superset of Y_S , i.e., $Y_T = \{Y_S, C + 1\}$, where $C + 1$ is the unknown class.

Variational Domain Disentanglement (VDD). The overview of the proposed VDD framework is presented in Fig. 1. In each batch, we sample data from each source domain and target domain and denote them as x for brevity. We use d as the domain label of x , and randomly sample a fake domain label d' that $d' \neq d$. The dual-branch encoder consists of a domain encoder $E_d(\cdot; \phi_d)$ and a sample encoder

¹<https://github.com/Jo-wang/VDD>

$E_s(\cdot; \phi_s)$ that produces a variational probability model $q_\phi(z|x, d)$. Here the variational parameters are $\phi = \{\phi_d, \phi_s\}$. The latent variable for the domain label, fake domain label and sample are $z_d, z_{d'}$ and $z_s \in \mathbb{R}^m$. We concatenate the $z_d, z_{d'}$ with z_s and feed them to the decoder network $G(\cdot; \theta)$ to reconstruct sample $\hat{x} = G([z_s; z_d])$ and a fake sample $\hat{x}' = G([z_s; z_{d'}])$. On top of the encoder, a classifier $h(\cdot)$ is trained to take z_s as input to make predictions. We will detail each component in the following sections.

3.2. Dual-branch Variational Autoencoders

The main challenge of the GMDA task is to learn a domain-agnostic model while avoiding negative transfer caused by the category shift and domain gap. The key idea is to separate the *domain-specific* information and the *domain-invariant* features that are only related to samples' semantics. VAEs [17] are generative models that jointly train both probabilistic encoder and decoder, wherein the encoder learns to generate the latent variable z following the pre-defined prior $p(z)$. In particular, to optimize the reconstructed output, we maximize the following evidence lower bound (ELBO),

$$\mathcal{L}_{\text{VAE}} = \mathbb{E}_{q_\phi(z|x)}[-\log(p_\theta(x|z))] + D_{\text{KL}}(q_\phi(z|x)||p(z)), \quad (1)$$

where z is the concatenation of the sampled vector z_s and z_d , i.e., $z = [z_s; z_d]$. The first term can be interpreted as a reconstruction loss $\int q_\phi(z|x) \times \|x - G(z)\|^2 dz$, which aims to recover the original image with the domain vector z_d and sample vector z_s . The second term calculates the KL-divergence, which penalizes the deviation of the latent feature z from the prior distribution $p(z)$. Without loss of generality, we use a Gaussian distribution as a prior.

3.3. Exemplar Learning

In order to decouple the domain features from input image, we additionally generate 'fake' reconstructed image $\hat{x}' = G(z')$ by feeding the concatenation of $z_{d'}$ and z_s , i.e., $z' = [z_s; z_{d'}]$ into the decoder. The generation of \hat{x}' is supervised by a novel *exemplar learning*: for each category c in each domain i , we randomly choose one sample as an exemplar v_i^c and store it in the exemplar pool $\mathcal{V} = \{v_i^1, \dots, v_i^C\}_{i=1}^N$. Then the corresponding exemplar is used as a ground-truth of the fake reconstructed image that shares the same class and domain label to calculate the reconstruction loss:

$$\mathcal{L}_{\text{exe}} = \mathbb{E}_{q_\phi(z'|v)}[-\log(p_\theta(v|z'))] + D_{\text{KL}}(q_\phi(z'|v)||p(z')), \quad (2)$$

where v stands for the selected exemplar that matches the class of x and the domain index of d' . The motivation of applying the exemplar learning is to (1) stabilize the image reconstruction, and the separation of domains and instances; (2) implicitly minimize the variance of the latent variable z and force it to be more correlated to the semantics, hereby improving the classification accuracy.

3.4. Disentangled Factor Learning

To achieve domain disentanglement and domain generalization with explainability, we employ *disentangled factor learning*. The key insight is to make domain features orthogonal to each other in the latent space, i.e., $z_{d_i} \perp z_{d_j}$ where z_{d_j} indicates the j -th dimension of the domain latent vector z_d . Each dimension of z_d is independent, so that the representations can potentially generalize to other unseen domains. To facilitate this, we substitute the KL-divergence terms in Eq.(1) and Eq.(2):

$$D_{\text{KL}}(q_\phi(z|x)||p(z)) = I_{\phi_d}(z_d; n) - \beta \mathcal{L}_{tc} - \xi \mathcal{L}_{dim}, \quad (3)$$

$$\begin{aligned} I_{\phi_d}(z_d; n) &= D_{\text{KL}}(q_{\phi_d}(z_d, n)||q_{\phi_d}(z_d)p(n)), \\ \mathcal{L}_{tc} &= D_{\text{KL}}(q_{\phi_d}(z_d)||\prod_j q_{\phi_d}(z_{d_j})), \\ \mathcal{L}_{dim} &= \sum_j D_{\text{KL}}(q_{\phi_d}(z_{d_j})||p(z_{d_j})), \end{aligned} \quad (4)$$

where n indicates the sample index of the x , and $p(n)$ is $\frac{1}{n}$. The index-code mutual information $I_{\phi_d}(z_d; n)$ is calculated between data variable and latent variable on the basis of empirical data distribution $q_{\phi_d}(z_d, n)$. \mathcal{L}_{tc} is the total correlation (TC) that measures the dependency between the variables so that reducing TC could benefit learning statistically independent factors in the data distribution. \mathcal{L}_{dim} is the dimension-wise KL-divergence that limits individual latent dimensions to deviate too far from their respective priors.

3.5. Online Pseudo Labeling

Aiming at improving the classification performance on the unlabeled target domain, we choose to perform batch-wise pseudo labeling, which helps propagate the knowledge from labeled source data to unlabeled target data. In particular, based on the prediction $\hat{p}(x) \in \mathbb{R}^{C+1}$ produced from the classifier for each target sample x ($x \sim D_T$), we assign the pseudo label \hat{y} by thresholding the confidence with δ_{known} and δ_{unk} . To be detailed,

$$\hat{y} = \begin{cases} \arg \max \hat{p}(x), & \text{if } \max \hat{p}(x) > \delta_{known} \\ C + 1, & \text{if } \max \hat{p}(x) < \delta_{unk} \\ \emptyset. & \text{otherwise} \end{cases} \quad (5)$$

After that, the pseudo labeled data is utilized to train the model in turn with the cross-entropy loss:

$$\mathcal{L}_{\text{pseudo}} = \mathbb{E}_{x \sim D_p} - \hat{y} \log \hat{p}(x), \quad (6)$$

where $D_p = \{(x_t, \hat{y}) | \hat{y} \neq \emptyset\}$ is defined as the set of pseudo labeled target data and the respective pseudo labels. To further remain the inter- and inner-relationship between classes and avoid overfitting, the soft entropy \mathcal{L}_t as applied as a regularizer on the target data:

$$\mathcal{L}_t = \mathbb{E}_{x \sim D_T} - \hat{p}(x) \log \hat{p}(x). \quad (7)$$

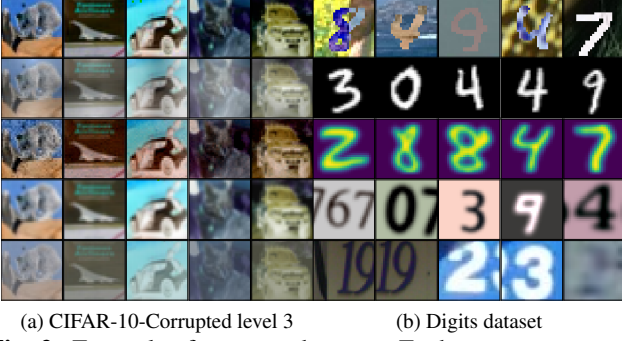


Fig. 2: Examples from two datasets. Each row represents a different domain.

While for the source data, cross-entropy loss \mathcal{L}_s is employed:

$$\mathcal{L}_s = \mathbb{E}_{x \sim D_S} - y \log \hat{p}(x). \quad (8)$$

3.6. Joint Optimization

To conclude, the overall objective of the proposed model is to minimize:

$$\mathcal{L} = \lambda \mathcal{L}_s + \mathcal{L}_t + \gamma \mathcal{L}_{VAE} + \alpha \mathcal{L}_{exe} + \mathcal{L}_{pseudo}. \quad (9)$$

4. EXPERIMENTS

4.1. Setup

Datasets. Experiments are performed on the following datasets: Digits, CIFAR-10-Corrupted [18]. Examples are shown in Fig. 2. Specifically, Digits dataset consists of five different domains includes MNIST-M [19] (mm), MNIST [20] (mt), USPS [21] (up), SVHN [22] (sv), and Synthetic Digits [19] (sy). CIFAR-10-Corrupted [18] is composed of 19 different noises as domains, each of which contains five levels of data that indicate noise intensity. Each level has eight classes. We randomly choose five domains, including frost (fro), fog (fo), contrast (co), defocus blur (def), and brightness (bri), of them and evaluate the performance by level 1 and level 3 data. We randomly choose half of the classes for each dataset as the unknown class.

Baselines. Since there is no previous setting exactly the same as ours, we apply the models include single-source methods such as MMD [23], CORAL [24] and DANN [19], multi-source approaches MSDA [10] and Ltc-MSDA [11]. They are further combined by open-set methods OSVM [25] and OSBP [26], as our baselines.

Evaluation Protocol. Three metrics are adopted, i.e., normalized accuracy for all classes (**OS**), normalized accuracy for the known classes only (**OS***), and **H-score**. It is worth noting that H-score is the fairest way to evaluate models' performance, as it balances the OS* and UNK [27].

Implementation Details. In terms of the model details, the domain encoder consists of one word embedding layer with the dimension of 512, followed by a linear layer to output the mean μ_d and standard deviation σ_d while the output dimension is set to 30 and 100 for Digits and CIFAR-10-Corrupted, respectively. The sample encoder is constructed by three convolutional layers with batch normalization and LeakyReLU and followed by two linear layers to output the latent representation of samples with the dimension of 2048 for all datasets. With the same basic residual block as ResNet, the decoder first feeds z into a linear layer, followed by one convolutional layer with ReLU as activation. After parsing the intermediate output into two sets of residual blocks, it goes through a convolutional layer with Sigmoid to produce the reconstructed image. The total number of training epoch M is 50 for Digits and 100 for others. The batch size of Digits is set to 32, and 20 for the CIFAR-10-Corrupted dataset. Adam is used as the optimizer with a weight decay of $5e^{-4}$. Following the settings in [19], the learning rate μ is initiated as 2×10^{-4} , decaying as the number of epoch increases. The dropout rate is set to 0.7. In \mathcal{L}_{VAE} , β is set to 6, and ξ is 1. The loss coefficient λ is set to 2 and γ is 1, instead, α is empirically defined in a progressive way: $\alpha = \frac{m}{2M}$, where m is the learning step. The threshold δ_{known} is empirically set to be 0.9, and δ_{unk} is 0.3 in online pseudo labeling.

4.2. Experimental Results

Quantitative Results. The results of the proposed method and the compared baselines are presented in Tables 1 and 2. It can be observed in the tables that the proposed method outperforms most baseline approaches. Taking the Digits dataset as an example, we have the following observations: Combined with the open-set methods, most existing frameworks perform similarly regardless of single- or multi-source domains, indicating that domain shift is not the core issue under the GMDA setting. In terms of the category shift, although OSVM is generally better than OSBP, it is sensitive to the chosen threshold, while there is no similar limitation for OSBP when holding the competitive results. Compared with all baselines, especially for the target USPS dataset, VDD achieves more than 7% improvement in terms of H-score. The main reason is that VDD can learn domain invariant representations by disentangling multiple source domains. In light of this, the predictions on the target domain can be confidently produced. The experimental outcomes performed on CIFAR-10-Corrupted shows that the proposed method can achieve the best performance in most cases, which further verifies the superiority of the VDD.

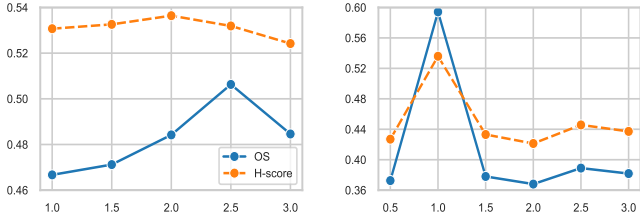
Qualitative Results. We provide some samples of the reconstructed and 'fake' reconstructed images in Fig. 4. After changing the domain embedding, the background style is changed accordingly, while the semantics remain the same.

Table 1: Recognition accuracies on the Digits benchmark.

Protocol	Method	$mt, up, sv, sy \rightarrow mm$			$mm, up, sv, sy \rightarrow mt$			$mm, mt, sv, sy \rightarrow up$			$mm, mt, up, sy \rightarrow sv$			$mm, mt, up, sv \rightarrow sy$		
		OS	OS*	H-score	OS	OS*	H-score	OS	OS*	H-score	OS	OS*	H-score	OS	OS*	H-score
Source Comb.	OSVM	0.4363	0.3696	0.4995	0.7344	0.7743	0.6327	0.7282	0.7778	0.5935	0.3476	0.2519	0.3861	0.5359	0.5333	0.5410
	OSBP [26]	0.4175	0.3869	0.4611	0.7983	0.8590	0.6281	0.8206	0.8564	0.7335	0.3708	0.3505	0.4024	0.4625	0.4459	0.4907
	MMD [23] + OSVM	0.4534	0.3879	0.5184	0.7349	0.7686	0.6452	0.7222	0.7691	0.5968	0.3722	0.2992	0.4257	0.5529	0.5610	0.5357
	CORAL [24] + OSVM	0.4500	0.3941	0.5118	0.7389	0.7755	0.6474	0.7321	0.7807	0.6013	0.3828	0.3102	0.4382	0.5449	0.5504	0.5334
	DANN [19] + OSVM	0.4617	0.4313	0.5066	0.7328	0.7642	0.6568	0.7257	0.7778	0.5823	0.4687	0.4756	0.4479	0.5544	0.5590	0.5449
Multi.	MSDA [10]+OSBP	0.4058	0.3267	0.4642	0.8230	0.8940	0.6390	0.7171	0.7289	0.6919	0.4106	0.3795	0.4545	0.3995	0.3331	0.4578
	Ltc-MSDA [11]+OSBP	0.4321	0.3307	0.4184	0.5902	0.5643	0.6326	0.7206	0.7317	0.6967	0.2598	0.2288	0.2949	0.3745	0.3408	0.4187
VDD		0.5942	0.6185	0.5359	0.8490	0.8965	0.7271	0.8303	0.8415	0.8066	0.4792	0.5345	0.3947	0.5659	0.5728	0.5626

Table 2: Recognition accuracies on the CIFAR-10-Corrupted benchmark. * indicates MSDA methods with OSBP.

Levels	Target Domain	fro	fo	def	bri	co
	Method	H-score	H-score	H-score	H-score	H-score
level 1	MSDA [10]*	0.2218	0.2984	0.2907	0.3057	0.2225
	Ltc-MSDA [11]*	0.1972	0.2143	0.2201	0.2295	0.2013
	VDD	0.3612	0.3525	0.3479	0.3608	0.3334
level 3	MSDA [10]*	0.2864	0.3666	0.4950	0.2125	0.3516
	Ltc-MSDA [11]*	0.2095	0.2194	0.2111	0.2123	0.2006
	VDD	0.3000	0.2956	0.3368	0.3823	0.2743



(a) α : coefficient of exemplar loss (b) γ : coefficient of β TC-VAE loss
Fig. 3: Parameter sensitivity of loss coefficients α and γ .

4.3. Parameter Sensitivity

We investigated the effect of hyperparameters on the performance of the VDD model, including the loss coefficients α and γ . α controls the importance of the reconstruction diversity, while γ weights the disentanglement process. We conduct two sets of parameter analysis by changing the value of α from 1 to 3.0, γ from 0.5 to 3.0, with the interval of 0.5, the results of which are plotted in Fig. 3. It shows that in [0.5, 2.5], the OS score of the proposed method grows as α increases. The H-score peak at about 0.536 where α is set to 2. While OS achieves the best when α is 2.5. These phenomena indicate that the exemplar loss applied contributes positively to the multi-source learning, yet amplifying the loss too much would hinder the classification learning. Compared with the results shown in Table 1, we can see that the best result comes from the progressively defined α , which implies dynamically adjusting the hyperparameter α could adapt the learning of the

Table 3: The ablation performance of the proposed VDD on the Digits dataset.

Method	$mt, up, sv, sy \rightarrow mm$		$mm, mt, up, sv \rightarrow sy$	
	OS	H-score	OS	H-score
GMDA w/o \mathcal{L}_{exe}	0.3767	0.4305	0.3463	0.3893
GMDA w/o disent	0.3920	0.4487	0.3246	0.3675
GMDA	0.5942	0.5359	0.5659	0.5626

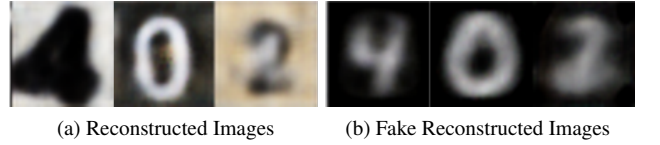


Fig. 4: Examples of reconstructed and fake reconstructed image on Digits dataset

objective better. The result on γ exhibits a similar tendency, demonstrating that balancing the importance of different components can yield better results. Furthermore, it exemplifies that when γ is 1, the performance is the best, as evidenced by OS and H-score consistently. At the best result achieved by adjusting γ , we discover that the global tendency of OS and H-score are almost consistent under the influence of different values of α and γ . It indicates the influence of disentanglement significance on the model is integral, impacted the classification performance of each domain simultaneously.

4.4. Ablation Study

By conducting an ablation study that evaluates variants of VDD, we dive deep into the effectiveness of the proposed domain disentanglement framework. (1) **GMDA w/o \mathcal{L}_{exe}** is the variant without the diversified reconstruction by fake domain label in Eq. (2); (2) **GMDA w/o disent** is the variant without VAE loss in Eq. (3). The experimental results are reported in Table 3, where it can be observed that the absence of any part could lead to performance reduction. The missing of reconstruction diversity (i.e., \mathcal{L}_{exe}) causes about 0.219 de-

crease of OS and 0.136 of H-score on target domain MNIST-M and Synthetic Digits while lacking disentanglement results in 0.222 and 0.137 reduction for OS and H-score respectively. In addition, the degradation for both GMDA w/o \mathcal{L}_{exe} and GMDA w/o disent are almost the same, meaning that diversifying the reconstruction with exemplar learning is as crucial as disentangling the feature in the latent space.

5. CONCLUSION

In this paper, we propose a Variational Domain Disentanglement framework, which aims to address the domain and category shift in a novel GMDA setting. We verify that the alignment problem of multiple domains could be solved by disentangling the domain feature in latent space. Specifically, we record that previous state-of-the-art can be beaten by our domain disentanglement model. The ablation study shows that both reconstruction diversity and disentanglement method play great significant roles in the final result. We will explore the more challenging and practical domain adaption problems in the future.

6. REFERENCES

- [1] Massimiliano Mancini, Lorenzo Porzi, Samuel Rota Bulò, Barbara Caputo, and Elisa Ricci, “Boosting domain adaptation by discovering latent domains,” in *CVPR*, 2018.
- [2] Yitong Li, Michael Murias, Geraldine Dawson, and David E. Carlson, “Extracting relationships by multi-domain matching,” in *NeurIPS*, 2018.
- [3] Han Zhao, Shanghang Zhang, Guanhang Wu, José M. F. Moura, João Paulo Costeira, and Geoffrey J. Gordon, “Adversarial multiple source domain adaptation,” in *NeurIPS*, 2018.
- [4] Yadan Luo, Zijian Wang, Zi Huang, and Mahsa Baktashmotlagh, “Progressive graph learning for open-set domain adaptation,” in *ICML*, 2020.
- [5] Zhuoxiao Chen, Yadan Luo, and Mahsa Baktashmotlagh, “Conditional extreme value theory for open set video domain adaptation,” in *MMAsia*, 2021.
- [6] Yadan Luo, Zi Huang, Zijian Wang, Zheng Zhang, and Mahsa Baktashmotlagh, “Adversarial bipartite graph learning for video domain adaptation,” in *MM*, 2020.
- [7] Zijian Wang, Yadan Luo, Zi Huang, and Mahsa Baktashmotlagh, “Prototype-matching graph network for heterogeneous domain adaptation,” in *MM*, 2020.
- [8] Yishay Mansour, Mehryar Mohri, and Afshin Rostamizadeh, “Domain adaptation with multiple sources,” in *NeurIPS*, 2008.
- [9] Ruijia Xu, Ziliang Chen, Wangmeng Zuo, Junjie Yan, and Liang Lin, “Deep cocktail network: Multi-source unsupervised domain adaptation with category shift,” in *CVPR*, 2018.
- [10] Xingchao Peng, Qinxun Bai, Xide Xia, Zijun Huang, Kate Saenko, and Bo Wang, “Moment matching for multi-source domain adaptation,” in *ICCV*, 2019.
- [11] Hang Wang, Minghao Xu, Bingbing Ni, and Wenjun Zhang, “Learning to combine: Knowledge aggregation for multi-source domain adaptation,” in *ECCV*, 2020.
- [12] Luyu Yang, Yogesh Balaji, Ser-Nam Lim, and Abhinav Shrivastava, “Curriculum manager for source selection in multi-source domain adaptation,” in *ECCV*, 2020.
- [13] Zhi Chen, Yadan Luo, Ruihong Qiu, Sen Wang, Zi Huang, Jingjing Li, and Zheng Zhang, “Semantics disentangling for generalized zero-shot learning,” in *ICCV*, 2021.
- [14] Alexander H. Liu, Yen-Cheng Liu, Yu-Ying Yeh, and Yu-Chiang Frank Wang, “A unified feature disentangler for multi-domain image translation and manipulation,” in *NeurIPS*, 2018.
- [15] Jinming Cao, Oren Katzir, Peng Jiang, Dani Lischinski, Daniel Cohen-Or, Changhe Tu, and Yangyan Li, “Dida: Disentangled synthesis for domain adaptation,” *CoRR*, 2018.
- [16] Pan Xiao, Bo Du, Jia Wu, Lefei Zhang, Ruimin Hu, and Xuelong Li, “TLR: transfer latent representation for unsupervised domain adaptation,” in *ICME*, 2018.
- [17] Diederik P. Kingma and Max Welling, “Auto-encoding variational bayes,” in *ICLR*, Yoshua Bengio and Yann LeCun, Eds., 2014.
- [18] Dan Hendrycks and Thomas G. Dietterich, “Benchmarking neural network robustness to common corruptions and perturbations,” in *ICLR*, 2019.
- [19] Yaroslav Ganin and Victor S. Lempitsky, “Unsupervised domain adaptation by backpropagation,” in *ICML*, 2015.
- [20] Yann LeCun, Léon Bottou, Yoshua Bengio, and Patrick Haffner, “Gradient-based learning applied to document recognition,” *Proceedings of the IEEE*, 1998.
- [21] John S. Denker, W. R. Gardner, Hans Peter Graf, Donnie Henderson, Richard E. Howard, Wayne E. Hubbard, Lawrence D. Jackel, Henry S. Baird, and Isabelle Guyon, “Neural network recognizer for hand-written zip code digits,” in *NeurIPS*, 1988.
- [22] Yuval Netzer, Tao Wang, Adam Coates, Alessandro Bissacco, Bo Wu, and Andrew Y Ng, “Reading digits in natural images with unsupervised feature learning,” *NeurIPS W*, 2011.
- [23] Arthur Gretton, Karsten M. Borgwardt, Malte J. Rasch, Bernhard Schölkopf, and Alexander J. Smola, “ta kernel two-sample tes,” *J. Mach. Learn. Res.*, 2012.
- [24] Baochen Sun, Jiashi Feng, and Kate Saenko, “Correlation alignment for unsupervised domain adaptation,” *CoRR*, 2016.
- [25] Lalit P. Jain, Walter J. Scheirer, and Terrance E. Boult, “Multi-class open set recognition using probability of inclusion,” in *ECCV*, 2014.
- [26] Kuniaki Saito, Shohei Yamamoto, Yoshitaka Ushiku, and Tatsuya Harada, “Open set domain adaptation by backpropagation,” in *ECCV*, 2018.
- [27] Silvia Bucci, Mohammad Reza Loghmani, and Tatiana Tommasi, “On the effectiveness of image rotation for open set domain adaptation,” in *ECCV*, 2020.